International Journal of Modern Physics B
© World Scientific Publishing Company

World Scientific
www.worldscientific.com

NUMERICAL MODELING OF DENDRITIC GROWTH IN ALLOY SOLIDIFICATION WITH FORCED CONVECTION

DONGKE SUN†, MINGFANG ZHU and SHIYAN PAN

Jiangsu Key Laboratory for Advanced Metallic Materials, Southeast University, Nanjing, 211189, China
†sundongke@gmail.com

DIERK RAABE

Max-Planck-Institut für Eisenforschung, Max-Planck-Street 1, Düsseldorf, 40237, Germany

A two dimensional (2D) cellular automaton (CA) - lattice Boltzmann (LB) model is presented to investigate the effects of forced melt convection on the solutal dendritic growth. In the model, the CA approach of simulating the dendritic growth is incorporated with the kinetic-based lattice Boltzmann method (LBM) for numerically solving the melt flow and solute transport. Two sets of distribution functions are used in the LBM to model the convective-diffusion phenomena during dendritic growth. After validating the model by comparing the numerical results with the theoretical solutions, it is applied to simulate the single and multi dendritic growth of Al-Cu alloys without and with a forced convection. The typical asymmetric growth features of convective dendrite are reproduced and the dendritic morphology is strongly influenced by melt convection. The simulated convective multi dendritic features by the present model are also compared with that by the CA-NS model. The present model is found to be more computationally efficient and numerically stable than the CA-NS model.

Keywords: Dendritic growth; lattice Boltzmann method; cellular automaton; melt convection.

1. Introduction

Melt convection is an unavoidable phenomenon during solidification. It strongly affects the dendritic morphology and hence the final properties of castings. Several numerical studies have been performed on the interaction of melt convection and dendritic growth in pure materials or alloys by incorporating the phase field (PF) methods[1], the level set (LS) methods[2] or the cellular automaton (CA) methods[3] with the solution of Navier-Stokes (NS) equations.

The lattice Boltzmann method (LBM)[4,5] is a new technique for simulating complex physic phenomena of fluid flows. Instead of the NS equations, the discrete Boltzmann equation is solved to compute the flow with collision models such as Bhatnagar-Gross-Krook (BGK). Researchers extended LBM to simulate melt flow in crystal growth because of its higher computational efficiency and better numerical stability than the conventional computational fluid dynamics. Miller et al.[6] and Medvedev et al.[7] developed PF-LBM coupled models to simulate the thermal dendritic growth with flow.

However, these models are usually focused on pure substance. Considering that LBM is originated from the lattice gas automata method that is actually a type of CA methods, it is natural to develop a model coupling CA and LBM to simulate dendritic growth of alloys in the presence of melt flow.

This paper presents a 2D CA-LBM model for modeling dendritic growth of binary alloys with forced convection. After validating the model by the comparisons between the simulated results and the theoretical predictions, numerical simulations are performed for single dendritic growth both in a static melt and in a flowing melt of an Al-4wt%Cu alloy. Then it is applied to model multi dendritic growth with convection and the results are compared with that simulated by the CA-NS model[3].

2. Model Description and Numerical Algorithms

The present model involves two essential features: the calculation of melt convection and solute transport by the LBM with a lattice BGK (LBGK) scheme[4,5] and the calculation of dendritic growth by a CA approach. Since the thermal diffusivity of Al-Cu alloys is about 4 orders of magnitudes larger than the solute diffusivity, the kinetics for dendritic growth can be assumed to be solute-transport-controlled. In the present work, for the sake of simplicity, the temperature field in the domain is considered to be uniform with a constant undercooling or cooling down from the liquidus with a cooling rate of 10*K*/*s*.

2.1. *Lattice Boltzmann method for melt flow and solute transport*

In the LBM model, the viscous flow behavior emerges automatically from the intrinsic particle streaming and collision processes by simulating the interaction of a limited number of particles. According to the BGK approximation[4], the LB equation (LBE) can be expressed as:

$$f_i(\mathbf{x}+\mathbf{e}_i\Delta t, t+\Delta t) - f_i(\mathbf{x},t) = -[f_i(\mathbf{x},t) - f_i^{eq}(\mathbf{x},t)]/\tau) \tag{1}$$

where $f_i(\mathbf{x}, t)$ is the particle distribution function (PDF) representing the probability of finding a particle at location $\mathbf{x}$ at time t. $\mathbf{e}_i$ is the velocity of the particles along the i-th directions. $f_i^{eq}(\mathbf{x}, t)$ is the equilibrium PDF (EPDF) and τ is the relaxation time. LBM can be modified to account for the solute transport due to convection and diffusion. Similar to that for the flow field calculation, the LBE for the solute field calculation can be read as[5]:

$$g_i(\mathbf{x}+\mathbf{e}_i\Delta t, t+\Delta t) - g_i(\mathbf{x},t) = -[g_i(\mathbf{x},t) - g_i^{eq}(\mathbf{x},t)]/\tau_D + S_i(\mathbf{x},t) \tag{2}$$

where $g_i(\mathbf{x}, t)$, $g_i^{eq}(\mathbf{x}, t)$ and τ_D are the PDF, the EPDF and the relaxation time for the solute field calculation, respectively. S_i is the source term related to the increased solute concentration ΔC due to the rejected solute during crystal growth. The fluid density ρ, the velocity $\mathbf{u}$ and the solute concentration C can be obtained by the following equations:

$$\rho = \sum f_i\,,\ \rho\mathbf{u} = \sum f_i\mathbf{e}_i\,,\ C = \sum g_i \tag{3}$$

The present work adopts the D2Q9 LBM model, i.e., the 9-velocity model in 2D space[4]. The space is discretized into a square lattice, and the discrete velocities are given

by $\mathbf{e}_{i=0}=(0,\ 0)c$, $\mathbf{e}_{i=1,2,3,4}=(\cos[\pi(i-1)/2],\ \sin[\pi(i-1)/2])c$ and $\mathbf{e}_{i=5,6,7,8}=\sqrt{2}\ (\cos[\pi(2i-9)/4],\ \sin[\pi(2i-9)/4])c$, here $c=\Delta x/\Delta t$ is the lattice speed and Δx is the lattice spacing. The EPDFs of the D2Q9 model are chosen to be:

$$f_i^{eq}(\mathbf{x},t)=w_i\rho[1+3(\mathbf{e}_i\cdot\mathbf{u})/c^2+4.5(\mathbf{e}_i\cdot\mathbf{u})^2/c^4-1.5\mathbf{u}^2/c^2] \tag{4}$$

$$g_i^{eq}(\mathbf{x},t)=w_iC[1+3(\mathbf{e}_i\cdot\mathbf{u})/c^2+4.5(\mathbf{e}_i\cdot\mathbf{u})^2/c^4-1.5\mathbf{u}^2/c^2] \tag{5}$$

where w_i are the weight coefficients given by $w_{i=0}=4/9$, $w_{i=1,2,3,4}=1/9$ and $w_{i=5,6,7,8}=1/36$. It has been proved that the NS equations and the convection-diffusion equations can be recovered with the LBEs by the Chapman-Enskog analysis. Thus, the relations between the flow relaxation time τ and the kinematic viscosity ν as well as between the diffusion relaxation time τ_D and the solute diffusivity D can be obtained by:

$$\nu=c^2\Delta t(2\tau-1)/6,\ D=c^2\Delta t(2\tau_D-1)/6 \tag{6}$$

2.2. *Cellular automaton method for the simulation of dendritic growth*

The kinetics of crystal growth controlled by the thermal, the solutal and the capillary contributions can be described by the Gibbs-Thomson equation:

$$V=\mu\cdot(T_l-T+m\cdot[C(t)-C_0]-\Gamma\cdot\mathrm{f}(\theta,\theta_0)\cdot\kappa(t)) \tag{7}$$

where V is the growth velocity of the solid-liquid (SL) interface, μ is the interface kinetic coefficient, T_l is the liquidus temperature, T is the melt temperature, m is the liquidus slope, C_0 is the initial concentration, and Γ is the Gibbs-Thomson coefficient. $\kappa(t)$ is the interface curvature which is calculated in the same manner as in the Ref.8. Here, $\mathrm{f}(\theta,\theta_0)$ is the function accounting for the anisotropy of the surface tension. For the fourfold symmetric crystal, it can be calculated by:

$$\mathrm{f}(\theta,\theta_0)=1-15\varepsilon\cos[4(\theta-\theta_0)] \tag{8}$$

where ε is the degree of anisotropy of the surface energy. θ_0 is the angle of the preferential growth direction with respect to the x-axis, and θ is the growth angle between the normal to the interface and the x-axis, which can be calculated according to solid fraction gradient at the SL interface with $\theta=\arctan(\partial_y\varphi/\partial_x\varphi)$. In an interface cell, the solid fraction increment $\Delta\varphi$ is evaluated by $\Delta\varphi=V\cdot\Delta t/\Delta x$ and the rejected solute amount ΔC is calculated by $\Delta C=C(1-k)\Delta\varphi$, here k is the solute partition coefficient. The source term S_i in Eq.(2) can thus be obtained according to $S_i=w_i\Delta C$.

3. Results and Discussion

Numerical simulations are performed in a 2-D domain $\{(x, y) \mid 0\le x\le L,\ 0\le y\le L\}$ full of the Al-Cu alloy melt with an initial concentration C_0 and uniform temperature $T=T_l-\Delta T$. Here, ΔT is the undercooling. Initially, one or several seeds with preferred orientations exist in the cavity. The undercooled melt flows into the cavity from the top boundary with a uniform velocity $\mathbf{u}(x,\ y)|_{y=L}=(0,\ U_{in})$ and flows out from the bottom boundary with $\partial_y u_y|_{y=0}=0$. For the flow calculation, the non-equilibrium extrapolation scheme[9] is used to

treat the inlet and outlet boundary conditions. Periodic boundary conditions are imposed on the two sides of horizontal walls. The solute field boundary conditions are prescribed as $\partial_x C|_{x=0,\,L}=0$ and $\partial_y C|_{y=0,\,L}=0$. The Schmidt number, defined as $Sc\equiv\nu/D$, is Sc=18.855. The flow relaxation time is chosen to be τ=1 and τ_D can be computed by Eq.(6) according to Sc. The dimensionless undercooling, length, time, growth velocity and flow velocity are used by rescaling the relative quantities with $\Delta T_0=|m|C_0(1-k)$, $d_0=\Gamma/\Delta T_0$, $t_0=d_0^2/D$, $V_0=D/d_0$, and $U_0=\nu/d_0$, respectively, where ΔT_0 is the unit undercooling and d_0 is the solutal capillary length. The kinetic coefficient is taken as μ=0.008 $m/(K\cdot s)$. Other parameters are taken form Ref.3.

3.1. *Model validation*

First, we validate the model for purely diffusive crystal growth using the Stefan problem that describes the diffusion-controlled crystal growth with a planar front[10]. The relevant analytical solution for the solid fraction evolution is given by $\varphi-\varphi_0=\lambda\sqrt{Dt}$, where φ_0 is the initial solid fraction and λ is a constant. The comparison with the simulation is given in Fig.1. As shown, the agreement is excellent.

Then we validate the simulation of convective dendritic growth with the analytical Oseen-Ivantsov solution[11] that provides a relationship among the growth Peclet number $Pe_c\equiv VR/(2D)$, the flow Peclet number $Pe_f\equiv UR/(2D)$, and the driving force of growth. For the concentration-driven growth, the driving force is the dimensionless supersaturation $\Omega\equiv(C_l^*-C^\infty)/[C_l^*(1-k)]$, where C_l^* is the interface equilibrium concentration at the upstream tip and C^∞ is the concentration far away from the tip. Figure 2 indicates that the simulated curve of Pe_c vs Pe_f is close to the profile predicted by the Oseen-Ivantsov solution.

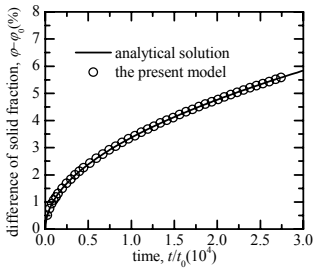

Fig. 1. The evolution of solid fraction for purely diffusive crystal growth with a planar interface.

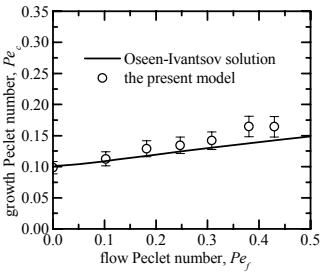

Fig. 2. The growth Peclet number as a function of the flow Peclet number for Ω=0.407.

3.2. *Single dendritic growth with melt convection*

Numerical experiments were done to study the effects of a forced flow on the growth process of a dendrite tip. Figure 3(a) illustrates the simulated evolution of the dendrites without flow and with a forced flow velocity of $U_{in}d_0/\nu$=0.005. It is found that the flow significantly influences the shape of dendrites. The flow takes the solute away from the

upstream region and thus the upstream concentration becomes lower. Since the liquidus slope m is a minus, the upstream solutal undercooling is increased higher than that on the downstream side. Accordingly, the growth velocity of the upstream tip is higher than that of the downstream tip. The upstream arm is thus rapidly developed while the downstream arm is retarded. The arm normal to flow grows slightly upwards because of the asymmetry of solute fluxes. As shown in Fig. 3(b), all tip velocities start from a large value and decrease very fast. After a transient period, the upstream tip reaches steady state growth. It indicates that the balance is established between dendritic growth and solute transport due to convection and diffusion in the front region of the upstream tip. The horizontal tip slowly reaches an approximately steady state after a relative longer time which is similar to that growing in a static melt. However, the downstream tip does not reach a complete steady state till the end of this simulation.

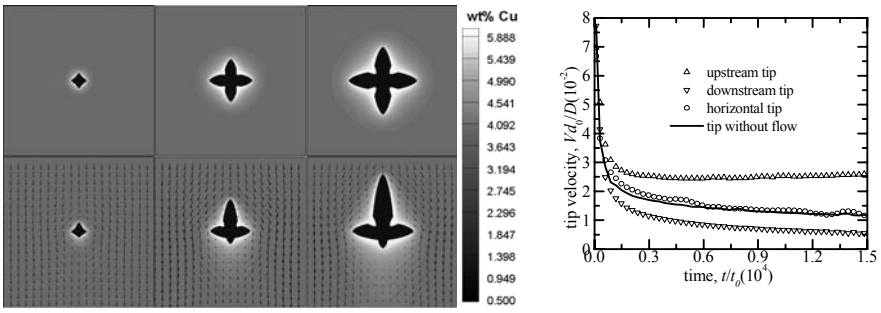

(a) (b)

Fig. 3. Evolution of (a) dendritic morphologies, φ=0.005, 0.030 and 0.065 from left to right and (b) dendrite tip velocities for an Al-4wt%Cu alloy growing at $\Delta T/\Delta T_0$=0.65 without flow and with an inlet flow velocity of $U_{in}d_0/\nu$=0.005 (θ_0=0, 400×400 grids with $\Delta x=4d_0$).

3.3. *Multi dendritic growth with melt convection*

The present model was also used to simulate the multi dendritic growth behavior. Figure 4 (a) indicates the simulated multi dendritic morphology of an Al-3wt%Cu alloy. Initially, six seeds with various preferred orientations were randomly placed in the domain. The melt temperature was assumed to be uniform and cooled down from the liquidus with a cooling rate of 10K/s. It is found that the flow plays a notable role in affecting growth behavior at the early stage of solidification. The asymmetric dendrite features are reproduced. As the dendrites grow close to each other, the flow gradually fades away in the inter-dendrites region and the effects of flow become less important. However, the final microstructure keeps the deflective features developed in the early stage of the solidification. Figure 4 (b) presents a comparison of the evolution of solid fraction calculated by the present model and the CA-NS model, where the melt flow is calculated by a NS solver. As shown, two curves coincide well before $\varphi\approx0.30$. In this simulation, the present model can model the multi dendritic growth till $\varphi\approx0.95$ whereas the CA-NS modeling was interrupted when $\varphi\approx0.30$ because the flow calculation by the NS solver

can't proceed when the solid fraction increases to higher value. Moreover, the calculating time by the present model with φ=0.30 is only about one-seventh of that by the CA-NS model. Accordingly, it can be concluded that the present model has the merits of better computational efficiency and numerical stability compared to the CA-NS model.

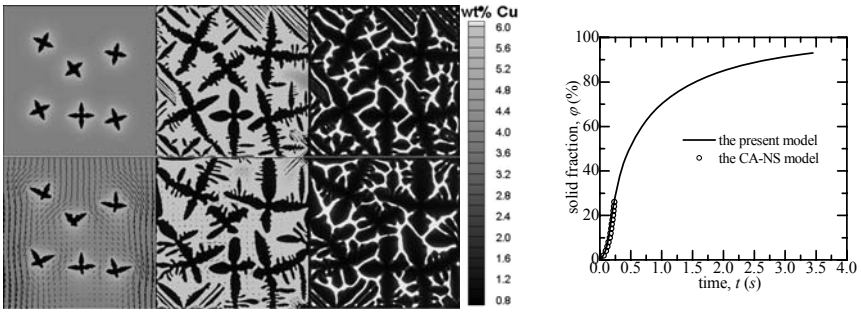

(a) (b)

Fig. 4. Evolution of (a) dendritic morphology without flow and with a flow velocity of U_{in}=0.001m/s, φ=0.05, 0.50 and 0.90 from left to right and (b) solid fraction for an Al-3wt%Cu alloy growing with a cooling rate of 10K/s (400×400 grids with Δx=1.0μm).

4. Conclusions

A LBM and CA coupled model has been developed to model dendritic growth with melt convection. The model is validated by the Stefan problem and the Oseen-Ivantsov solution. It is then applied to simulate single and multi dendritic growth of Al-Cu alloys both in a static melt and with a forced flow. The present model exhibits the quantitative and efficient capabilities. Moreover, it presents a better computational efficiency and numerical stability than the CA-NS model in simulating convective dendritic growth.

Acknowledgments

This work was supported by NSFC (50671025) and RFDP of China (20070286021).

References

1. X. Tong, C. Beckermann, A. Karma, Q. Li, *Phys. Rev. E*, **63**, 061601 (2001).
2. L. Tan, N. Zabaras, *J. Comput. Phys.*, **211**, 36 (2006).
3. M. F. Zhu, S.Y. Lee, C.P. Hong, *Phys. Rev. E*, **69**, 061610 (2004).
4. Y. Qian, D. d'Humières, P. Lallemand, *Europhys. Lett.*, **17**, 479 (1992).
5. B. Deng, B. C. Shi, G. C. Wang, *Chin. Phys. Lett.*, **22**, 267 (2005).
6. W. Miller, I. Rasin, F. Pimentel, *J. Cryst. Growth*, **266**, 283 (2004).
7. D. Medvedev, T. Fischaleck, K. Kassner, *J. Cryst. Growth*, **303**, 69 (2007).
8. L. Belteran-Sanchez, D. M. Stefanescu, *Metall. Mater. Trans. A*, **35**, 2471 (2004).
9. Z. L. Guo, C. G. Zheng, B. C. Shi, *Chin. Phys.*, **11**, 366 (2002).
10. H. B. Aaron, D. Fainstein, G. R. Kotler, *J. Appl. Phys.*, **41**, 4404 (1970).
11. Ph. Bouissou, P. Pelce, *Phys. Rev. A*, **40**, 6673 (1989).